Aust. J. Phys., 1988, 41, 549–61

Spectroscopic Studies of the Energy Levels of the Nd^{3+} Ion in Single Crystals of $SrO.6Al_2O_3$

H. Tajalli

Department of Physics, University of New England,
Armidale, N.S.W. 2351, Australia.
Permanent address: Physics Department, University of Tabriz,
Tabriz 51664, Iran.

Abstract

A detailed study of the polarised absorption and fluorescence spectra and the selective excitation spectra of the Nd^{3+} ion in the $SrO.6Al_2O_3$ host lattice was carried out over the temperature range 4·2 to 500 K. The empirical energy level schemes were determined for two dominant sites of Nd^{3+} in $SrO.6Al_2O_3$ up to 20 000 cm^{-1}. The intensity, linewidth and thermal shifts of the transition lines with $4f^3$ configuration were investigated. The vibrational transitions of $Nd^{3+}:SrO.6Al_2O_3$ were also investigated using Raman spectroscopy. The results of the study provide information on the suitability of $Nd^{3+}:SrO.6Al_2O_3$ as a solid state laser material.

1. Introduction

The triply charged ion of neodymium was one of the rare earth ions used in the early stages of development of the solid state laser, and remains as probably the most useful element of this group. Because of the distribution of allowable energy levels, due to a large L–S splitting ($\sim$2000 cm^{-1}) and a small crystal field splitting ($\sim$200 cm^{-1}), leading to a four-level laser system with low threshold energy, this ion has been incorporated satisfactorily in many glasses and crystalline matrices. Only a few of these matrices have been successfully developed, leading to efficient laser actions at 1·06 μm, corresponding to transitions between Stark split levels of the $^4F_{3/2}$ and $^4I_{11/2}$ L–S multiplet of the free Nd^{3+} ion.

It seems likely that a thorough study of mixed oxides could provide valuable information on the choice of solid state laser material (Koningstein and Geusic 1964; Massey and Yarborough 1971; Lindop and Goodwin 1973; Arsenev *et al.* 1980; Bagdasarov *et al.* 1983; Zharikov *et al.* 1984; Schearer *et al.* 1986). The mixed oxide crystal of $SrO.6Al_2O_3$ doped with neodymium emits an intense luminescence. In addition to this property, its intrinsic hardness, chemical imperviousness and high optical quality are of considerable interest in the selection of solid state laser material.

In this paper, a detailed study of the optical spectrum of Nd^{3+} in $SrO.6Al_2O_3$ and a construction of the energy level diagrams of Nd^{3+} ion in this crystal is reported.

0004-9506/88/040549$03.00

2. Experimental Procedure

(a) Preparation of Crystals

Single crystals of $SrO.6Al_2O_3$ were grown by the Czochralski technique from the melt of 0·5 and 1·0 at.% Nd^{3+} concentrations. The exact concentration of Nd^{3+} in these crystals was determined by X-ray fluorescence using powder standards, and found to be 0·07±0·01 and 0·34±0·03 at.% for the crystals grown in melts of 0·5 and 1·0 at.% Nd^{3+} concentration respectively. The crystal $SrO.6Al_2O_3$ belongs to the hexagonal systems with space group $P63/mmc$ and has the unit cell parameters of $a = b = 5·5620±0·0022$ Å and $c = 21·972±0·005$ Å (Braun 1957).

Crystal samples used for absorption studies were cut as slabs and their faces polished. The thickness of these slabs varied from 0·3 to 11·2 mm. The thinnest of these crystals was used to achieve the best resolution and the sharpest lines for transitions originating from the lowest $^4I_{9/2}$ crystalline Stark components, and the thickest crystal was used to bring out weaker transitions.

(b) Optical Techniques

The assignment of energy levels to a particular ion site in a matrix, where several ionic sites are available, involves the use of a number of techniques, including (i) absorption spectroscopy, (ii) fluorescence spectroscopy, (iii) polarisation spectroscopy, (iv) excitation spectroscopy and (v) Raman spectroscopy.

Absorption spectra at 4·2, 77 and 290 K were recorded in the near infrared and visible regions using either a tungsten or tungsten–halogen source with a Hilger Monospek 600 scanning monochromator, fitted with a 300 lines per mm grating blazed in the first order at 1 μm and with reciprocal dispersion of 26·7 Å mm^{-1}. A minimum spectral slit width of 1·2 Å was used. Optical detection was carried out using either a S1 photomultiplier cooled to 77 K or a PbS cell. Mechanical light modulation at 700 Hz was followed by a phase sensitive detector (PSD) system. Spectra were recorded simultaneously on a chart recorder and in digital form on punched tape. A Hilger-800 spectrophotometer with NaCl optics was used to record the absorption spectra in the infrared.

Fluorescence spectra were recorded by using excitation with either an HBO 200 high pressure mercury lamp or a quartz–halogen lamp directed onto one face of the crystal, and by detecting the fluorescence radiation at 90° through an RG780 filter to remove scattered radiation.

The arrangement of the optical apparatus for selective excitation was similar to that used for fluorescence spectroscopy; the only difference being the use of a Bausch–Lamb monochromator fitted with a 600 lines per mm grating blazed in the first order at 300 nm with linear dispersion of 33 Å mm^{-1}, added in the front of the 500 W high pressure mercury lamp. This monochromator selects bands with different bandwidth from the continuous spectrum of the excitation source used to excite the crystal. The Raman spectra were obtained using (356·4 nm) excitation from a krypton ion laser. The scattered light was dispersed with a Jobin–Yvon Hg_2 spectrometer, fitted with a holographic grating. A cooled S-11 photomultiplier was used for detection, followed by a Nicolet 1074 multichannel analyser. Recorded spectra were processed on an ICL 4130 computer to obtain central wavelength, peak intensity and linewidth of the individual lines in the overlap spectrum, using least-squares fits and assuming either Lorentzian or Gaussian lineshapes. Both the observed spectra and those that

were computed using the calculated parameters were displayed for comparison on the computer graph plotter.

3. Spectra

(a) Absorption Spectrum

The energy levels of the Nd^{3+} ion, with $4f^3$ configuration, have been tabulated for a number of host lattices (Dieke and Crosswhite 1963; Koningstein and Geusic 1964; Lindop and Goodwin 1973). These energy levels arise from the crystal field splitting and the J-manifold within the 4f shell, extending up to 40 000 cm^{-1}. Absorption transitions give rise to the crystal field splitting group that start from the levels of the ground ($^4I_{9/2}$) multiplet and terminate in various excited levels. These transitions in the absorption spectrum of Nd^{3+} in $SrO.6Al_2O_3$ at 4·2 K originate predominantly from the lowest level of the $^4I_{9/2}$ manifold. The position of the excited state is thus directly obtained from absorption at 4·2 K.

The absorption spectrum of Nd^{3+} in $SrO.6Al_2O_3$ was investigated from 0·5 μm in the visible region to 5·5 μm in the infrared, the transmission limit of $SrO.6Al_2O_3$. The observed infrared absorption spectra are discussed in the two subsections below.

The positions of lines in the spectra depend on temperature. The temperature shifts, however, are small (a few cm^{-1}) towards longer wavelengths when the temperature varies from 77 to 290 K.

Polarisation of all transitions within the $4f^3$ configuration were obtained at 77 K. From comparison of the axial and transverse spectra it was determined that all the lines observed in the range up to 800 nm were from electric dipole transitions.

Infrared absorption spectrum of Nd^{3+} in $SrO.6Al_2O_3$. Three groups of transitions have been observed in the absorption spectrum at 77 K between 1900 and 6600 cm^{-1}. These originate from the lower levels of the $^4I_{9/2}$ state and terminate on crystal field levels of the $^4I_{11/2}$, $^4I_{13/2}$ and $^4I_{15/2}$ manifolds. The transitions to the $^4I_{11/2}$, $^4I_{13/2}$

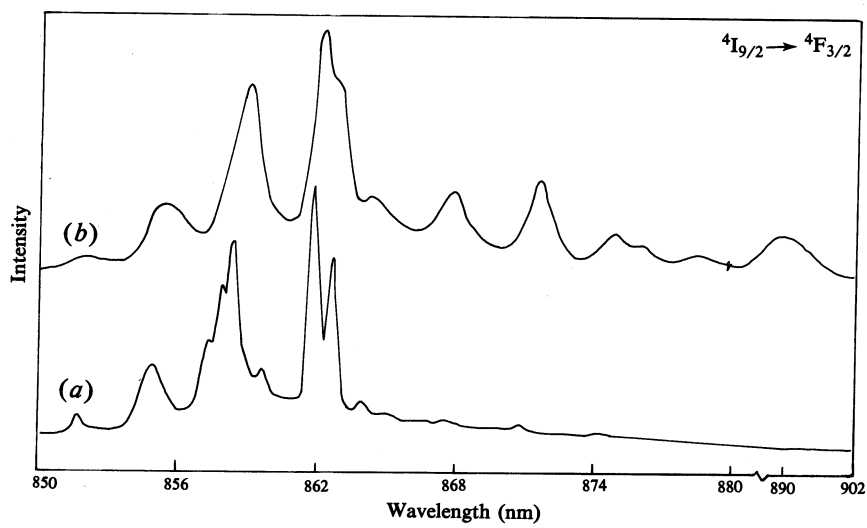

Fig. 1. Absorption spectrum of Nd^{3+} : $SrO.6Al_2O_3$ at the temperatures (*a*) 4·2 K and (*b*) 290 K.

Table 1. $Nd^{3+}:SrO.6Al_2O_3$ absorption at 77 K for $^4I_{9/2} \longrightarrow {}^4F_{5/2}$ and $^2H_{9/2}$

Wavelength (nm in air)	Wavenumber (cm^{-1} in vacuum)	Polarisation[A]	Linewidth (nm)
805.6	12414.0	SP	0.39
803.6	12445.0	S	0.34
802.9	12455.0	SP	0.50
801.5	12476.5	SP	0.56
800.2	12497.0	P	0.58
799.9	12501.5	SP	0.41
798.8	12519.0	SP	0.34
798.0	12531.0	SP	0.38
797.1	12545.0	S	0.50
796.9	12549.0	SP	0.54
796.3	12558.0	SP	0.45
796.1	12562.0	S	0.40
794.6	12584.0	SP	0.66
794.2	12592.0	S	0.52
793.8	12597.0	SP	0.54
793.1	12609.0	P	0.38
792.4	12620.0	SP	0.50
791.8	12630.0	SP	0.42
790.7	12647.0	P	0.56
790.2	12656.0	SP	0.44
798.8	12661.5	SP	0.38
789.4	12668.0	S	0.32
788.2	12687.0	S	0.66
787.5	12699.0	SP	0.53
787.1	12705.0	SP	0.45
786.7	12711.0	SP	0.58
786.2	12719.0	S	0.49
784.7	12745.0	SP	0.73
784.3	12750.0	P	0.63
781.5	12796.0	S	0.62
789.9	12805.0	SP	0.84
779.5	12830.0	S	0.62
778.5	12846.0	S	0.63
778.1	12852.5	SP	0.70
770.9	12972.0	SP	0.50
770.5	12978.5	SP	0.72
765.0	13072.0	SP	0.87
764.6	13079.0	SP	0.67

[A] S and P represent σ and π polarisations respectively.

and $^4I_{15/2}$ states are found between 1900–2300, 3950–4300 and 5750–6600 cm^{-1} respectively.

Near infrared and visible absorption spectrum of Nd^{3+} in $SrO.6Al_2O_3$. In the near infrared, a group of transitions has been observed in the absorption spectrum at 4·2 and 77 K for transitions from $^4I_{9/2}$ to $^4F_{3/2}$ between 11200 and 11750 cm^{-1}. Fig. 1 shows the absorption spectrum for transitions from levels of the $^4I_{9/2}$ manifold to levels of the $^4F_{3/2}$ manifold at temperatures 290 and 4·2 K. The two terms $^4F_{3/2}$ and $^2H_{9/2}$ are very close to each other in L–S splitting, and their Stark states mix together to form a broad absorption band. A large number of absorption transitions from the $^4I_{9/2}$ term to the $^4F_{5/2}$ and $^2H_{9/2}$ terms were detected. They were strong, sharp and very close to each other. In Table 1 the wavelengths, energy differences, polarisations and linewidths of only strong lines of this absorption spectrum are given at 77 K. Two terms of $^4F_{7/2}$ and $^4S_{3/2}$ are also very close to each other. Fig. 2 shows the σ and π polarised spectra along with the axial spectrum for transitions between the crystalline Stark component of $^4I_{9/2}$ to $^4F_{7/2}$ and $^4S_{3/2}$ at 77 K. The transitions from the ground ($^4I_{9/2}$) to levels of the $^4F_{9/2}$ manifold are observed between 14 600 and 15 100 cm^{-1}. Only seven absorption lines were observed for transitions from $^4I_{9/2}$ to $^2H_{11/2}$ at 77 K and this decreased to four at 4·2 K. Transitions from the ground state ($^4I_{9/2}$) to levels of the $^2G_{7/2}$ and $^4G_{5/2}$ manifolds were recorded between 17 100 and 17 660 cm^{-1}. The absorption spectrum of $^4I_{9/2}$ to $^4G_{7/2}$ and $^4G_{9/2}$ at 77 K was found to contain a large number of lines, these transitions occurring between 18 900 and 19 950 cm^{-1}.

(b) Fluorescence Spectrum of Nd^{3+} in $SrO.6Al_2O_3$

Fluorescence spectra were observed for transitions from the $^4F_{3/2}$ manifold to the three lowest ^4I multiplets. The excitation induced by visible radiation produces transitions from the ground state ($^4I_{9/2}$) to higher states. A multiphonon de-excitation process to the $^4F_{3/2}$ level then takes place, followed by fluorescent transitions to the $^4I_{13/2}$, $^4I_{11/2}$ and $^4I_{9/2}$ levels. The measured wavelengths, and linewidths of each observed line are listed in Table 2 for $^4F_{3/2} \rightarrow {}^4I_{9/2}$, $^4F_{3/2} \rightarrow {}^4I_{11/2}$ and $^4F_{3/2} \rightarrow {}^4I_{13/2}$ at 77 K. Column 3 of this table gives the relative peak height of lines, normalised to the strongest line in the $^4F_{3/2} \rightarrow {}^4I_{11/2}$ transition at 9538 cm^{-1}. Fig. 3 illustrates the fluorescence spectrum of $^4F_{3/2} \rightarrow {}^4I_{11/2}$ at 77 and 290 K.

No fluorescence was observed for $^4F_{3/2} \rightarrow {}^4I_{15/2}$ transitions.

(c) Raman Spectrum

Some weak lines were detected in the absorption and fluorescence spectra, on either side of the strong transitions. These were separated in wavenumber from the strong lines by 93, 143, 205 and 433 cm^{-1}. These lines were observed in most of the absorption groups, but could not be identified as transitions between the crystalline Stark components of the $^4I_{9/2}$ term and other excited terms. In the absorption spectrum of $^4I_{9/2} \rightarrow {}^2H_{9/2}$ and $^4F_{5/2}$ at 4·2 K, in addition to the abovementioned lines, further weak lines with wavenumber separations of 313, 334, 395, 424, 452 and 489 cm^{-1} from the strong absorption transitions of 12662, 12657, 12652 and 12461 cm^{-1} were detected on the short wavelength side. They could not be electronic transitions, because the splitting of the $^2H_{9/2}$ and $^4F_{5/2}$ levels cannot be as great as this, whatever the point group symmetry of the surrounding ion in the crystal. It is suggested that these weak lines may be due to vibrational transitions of the crystal lattice, coupling with the main electronic transitions.

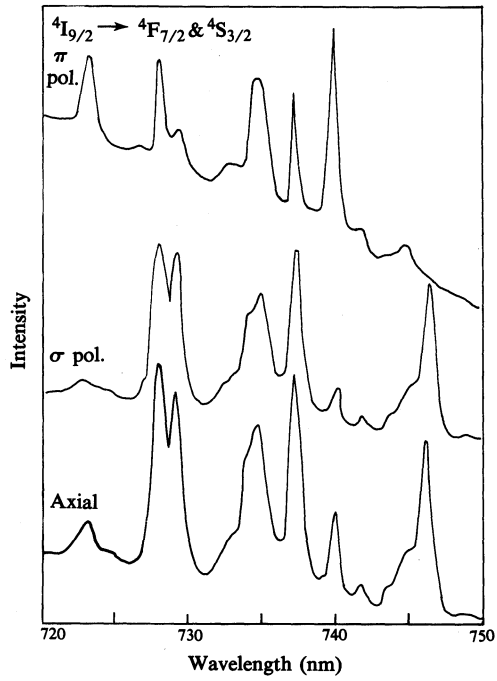

Fig. 2. Absorption spectrum of $Nd^{3+}:SrO.6Al_2O_3$ at 77 K, showing the σ and π polarised and the axial spectra.

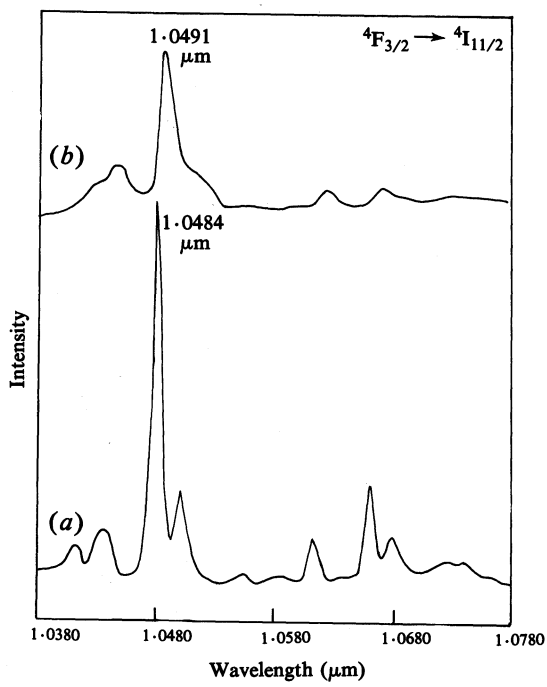

Fig. 3. Fluorescence spectrum of $Nd^{3+}:SrO.6Al_2O_3$ at the two temperatures (*a*) 77 K and (*b*) 290 K.

Table 2. Energy, linewidth and relative intensities of the strongest fluorescence lines of Nd^{3+} in $SrO.6Al_2O_3$ at 77 K

Energy (μm)	Linewidth (nm)	Intensity relative	Energy (μm)	Linewidth (nm)	Intensity relative
		Transitions $^4F_{3/2} \longrightarrow {}^4I_{9/2}$			
.9021	1.41	5.9	.8703	0.85(1.80)	16.5
.8987	1.95	76	.8664	1.10	8.5
.8767	.80	3.4	.8631	0.73(1.70)	3.5
.8762	.87	3.4	.8619	0.85(1.95)	9.5
.8747	.92(1.50)	10.2	.8611	0.83(1.40)	14.1
.8734	1.5(1.80)	11.2	.8580	0.76	3.0
		Transitions $^4F_{3/2} \longrightarrow {}^4I_{11/2}$			
1.0410	.72	7.0	1.0551	0.70	4.0
1.0415	.72	10.0	1.0610	0.86(1.50)	11.0
1.0430	.75	11.5	1.0658	1.10(1.50)	25.1
1.0435	.78(2.00)	10.5	1.0678	1.16	10.8
1.0484	.65(1.45)	100.0	1.0719	1.10	4.5
1.0502	.75	20.0	1.0744	1.0	4.7
1.0513	.80	9.0			
		Transitions $^4F_{3/2} \longrightarrow {}^4I_{13/2}$			
1.3029	1.26	3.7	1.3479	1.05	5.1
1.3045	1.06	13.0	1.3629	0.90	4.8
1.3305	1.30	5.0	1.3652	1.10	4.6
1.3370	1.35	4.1	1.3729	0.70	5.2
1.3382	1.20	3.7	1.3749	1.20	5.1
1.3437	1.52	4.5	1.3829	1.20	6.2
1.3443	1.30	4.5	1.3852	1.40	3.7

[A] Linewidths in parentheses are at 290 K.

In an attempt to confirm this suggestion, the vibrational modes of the crystal of Nd^{3+} in $SrO.6Al_2O_3$ were studied using Raman spectroscopy at 290 K. Table 3 presents the measured frequencies of 21 active Raman modes of Nd^{3+} in $SrO.6Al_2O_3$ at 290 K. This spectrum (Fig. 4) shows marked similarities with that of corundum (α, Al_2O_3) (Porto and Krishnan 1967; Askin *et al.* 1968) in the wavenumber range $>300\ cm^{-1}$. This is to be expected since the Al_2O_3 molecular unit is common to both crystals. There are vibrational modes which may, perhaps, be associated with the vibration of the heavy Sr ion.

Table 3. Raman lines of $Nd^{3+}:SrO.6Al_2O_3$ at room temperature

Wavenumber (cm^{-1})	Wavenumber (cm^{-1})	Wavenumber (cm^{-1})
80	396	648
140	428	678
234	454	730
280	486	758
320	528	804
334	488	816
344	628	868

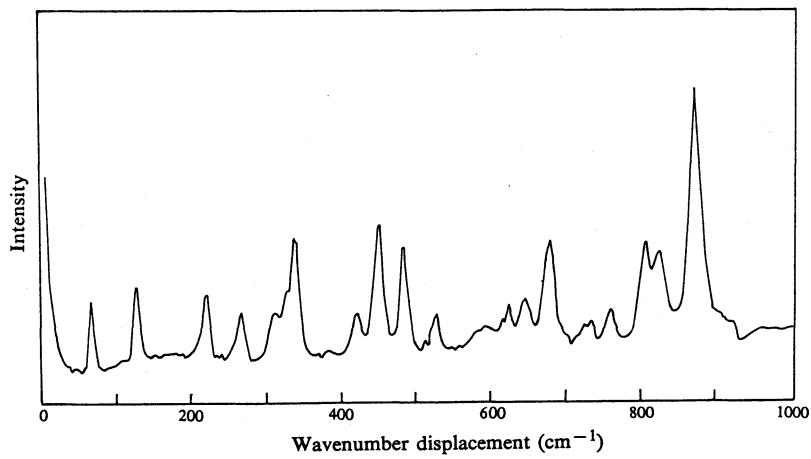

Fig. 4. Raman spectrum of $Nd^{3+}:SrO.6Al_2O_3$.

The Raman spectral lines were compared with the weak lines mentioned above. Apart from the 93 and 205 cm^{-1} lines, all appear to be nearly the same as the Raman frequencies. This supports the suggestion that the transitions are of a vibrational nature. It is possible that the 93 and 205 cm^{-1} lines are associated with electronic transitions of sites with different group symmetries from the two dominant sites considered, since the abovementioned weak lines are not far apart from the other electronic transitions. Further study will be required to verify this suggestion.

4. Discussion and Interpretation of the Spectra

A large number of absorption and fluorescence lines were found in the spectra of Nd^{3+} in $SrO.6Al_2O_3$; many more than would be expected from one site, suggesting the presence of more than one site for the Nd^{3+} ion. The observed spectra suggest two dominant sites having different symmetries. This has generally been the case for laser materials incorporating a trivalent rare earth ion in a divalent lattice (Toledano 1972; Ambrazyavichyus *et al.* 1981; Hayhurst *et al.* 1982). The reason for this multiplicity of sites could be due to charge compensation, or the substitution of

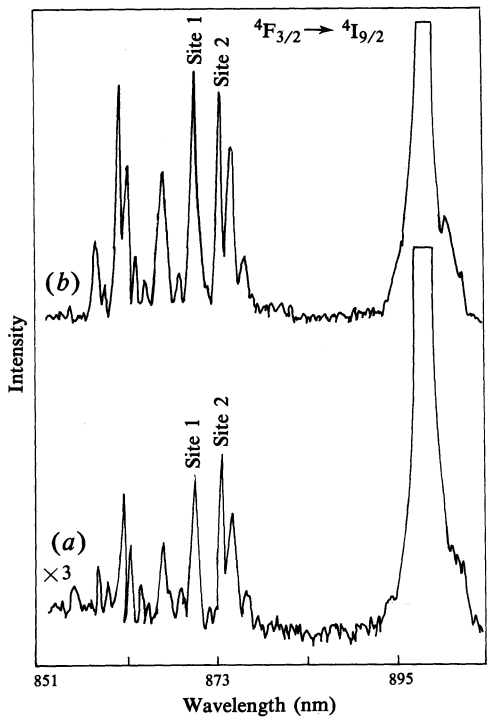

Fig. 5. Fluorescence spectrum for selective excitation: (*a*) for excitation with linewidth of 11 Å and (*b*) for excitation with linewidth of 18 Å. The lower spectrum has been magnified by 3.

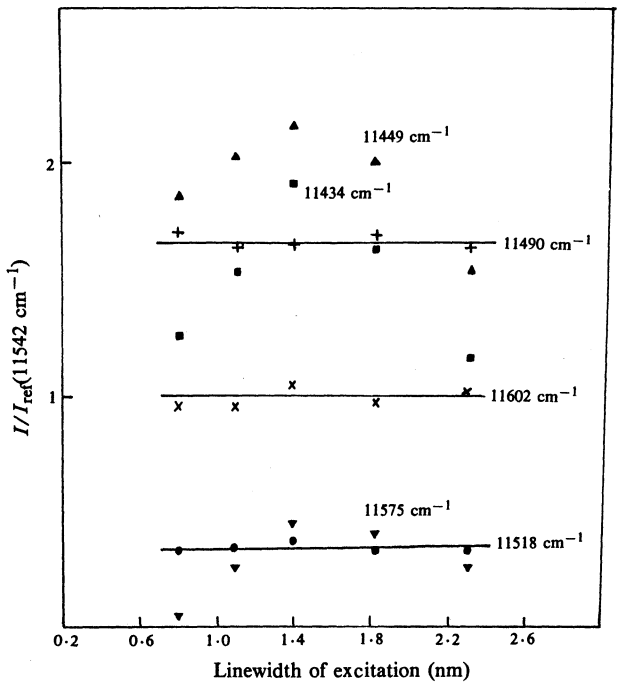

Fig. 6. Variation of the intensity of fluorescence transitions as a function of the linewidth of excitation.

Table 4. Energy levels of $Nd^{3+}:SrO.6Al_2O_3$ in cm^{-1} (up to 20000 cm^{-1}) for the two dominant sites at 77 K, with probable accuracy of 1 cm^{-1}

Site 1	Site 2	Manifold	Label	Number of Stark levels
0	0			
15	37			
85	162	$^4I_{9/2}$	Z	5
113	264			
241	484			
2051	2091			
2064	2115			
2179	2188	$^4I_{11/2}$	Y	6
2196	2284			
2251	2315			
2294	2381			
4086	3947			
4123	3989			
4167	4023	$^4I_{13/2}$	X	7
4183	4122			
4318	4171			
4371	4288			
4383	4329			
6054	6190			
6075	6281			
6237	6307			
6243	6344	$^4I_{15/2}$	W	8
6322	-			
6433	-			
-	-			
-	-			
11601	11612	$^4F_{3/2}$	R	2
11654	11697			
12593	12549			
12602	12620	$^4F_{5/2}$		
12641	12661			
12651	12699	&	S	8
12722	12745	$^2H_{9/2}$		
12791	12829			
12801	12994			
12975	13072			

Table 4. (*Continued*)

Site 1	Site 2	Manifold	Label	Number of Stark levels
13461	13496	$^4F_{7/2}$		
13458	13528			
13576	13655	&		
13636	13664	$^4S_{3/2}$	A	6
13724	13764			
13789	13844			
14864	14697			
14880	14715			
14902	14832	$^4F_{9/2}$	B	5
14943	14935			
14958	15068			
16042	15974			
-	16098	$^2H_{11/2}$	C	5
-	16228			
17204	17135			
17220	17259			
17267	17299	$^4G_{5/2}$		
17343	17394	&	D	7
17359	17469	$^2G_{7/2}$		
17446	17550			
17469	17657			
19017	18971			
19068	19107			
19157	19209	$^4G_{7/2}$	E	4
19227	19286			
19489	19433			
19520	19463			
19562	19699	$^4G_{9/2}$	F	5
19631	19792			
19751	19853			